

Supporting Materials:

Trapped intermediates in crystals of the FMN-dependent oxidase PhzG provide insight into the final steps of phenazine biosynthesis

Ningna Xu^{ab}, Ekta Gahanji Ahuja^{bc}, Petra Janning^d, Dmitri Valeryevich Mavrodi^e, Linda S. Thomashow^f and Wulf Blankenfeldt^{abg*}

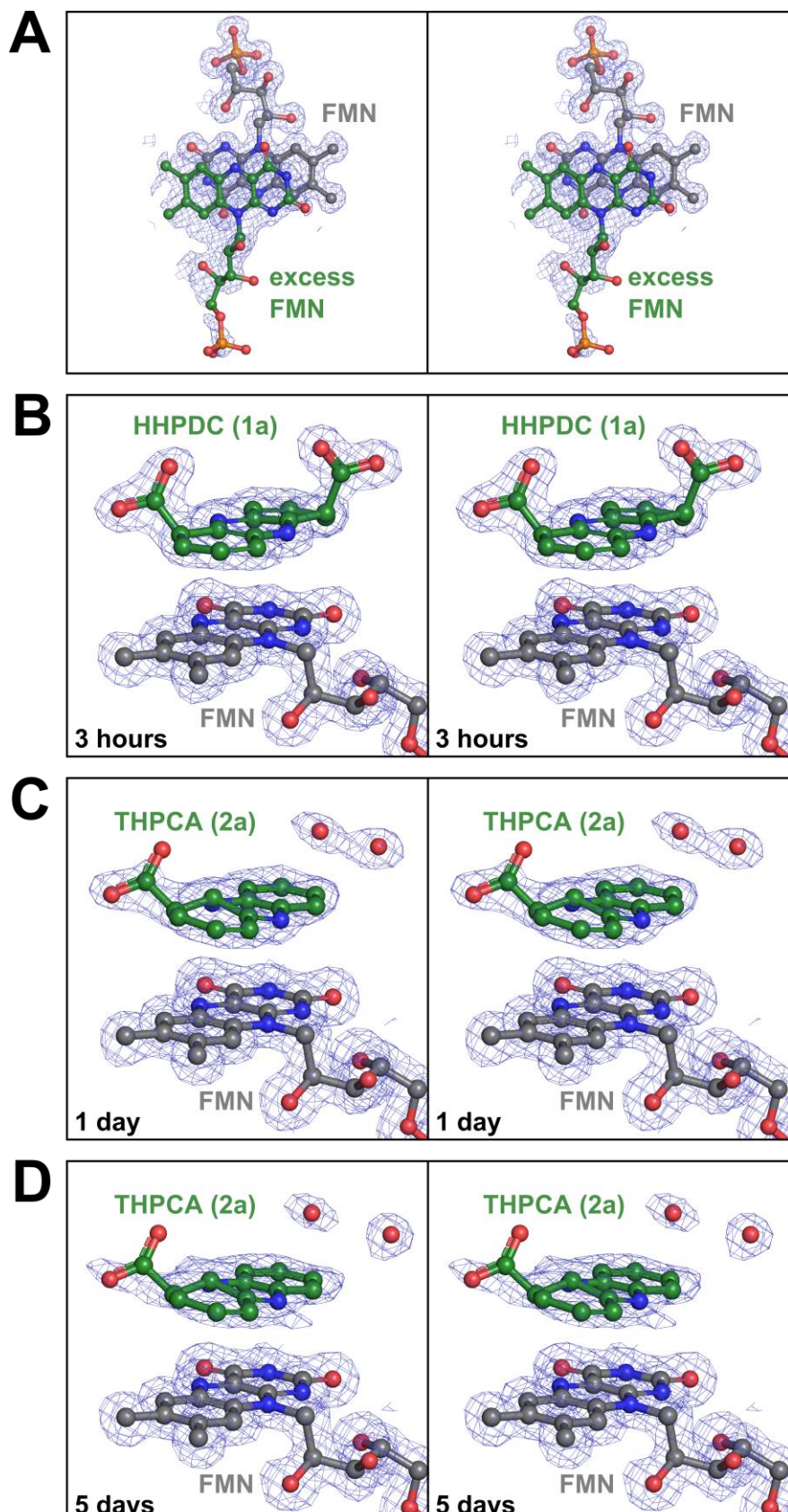
^aLehrstuhl für Biochemie, Universität Bayreuth, Universitätsstraße 30, Bayreuth, 95447, Germany,

^bPhysikalische Biochemie, Max-Planck-Institut für Molekulare Physiologie, Otto-Hahn-Straße 11,

Dortmund, 44227, Germany, ^cMithros Chemicals Pvt. Ltd., IKP Knowledgepark, Turkapally, Hyderabad, Andhra Pradesh, 500078, India, ^dChemische Biologie, Max-Planck-Institut für Molekulare Physiologie, Otto-Hahn-Straße 11, Dortmund, 44227, Germany, ^eDepartment of Plant Pathology, Washington State University, Pullman, Washington, WA 99164-6430, United States, ^fRoot Disease and Biological Control Research Unit, Agricultural Research Service, USDA-ARS, Pullman, Washington, WA 99164-4234, United States, and ^gBayreuther Zentrum für Molekulare Biowissenschaften (BZMB), Universität Bayreuth, Germany

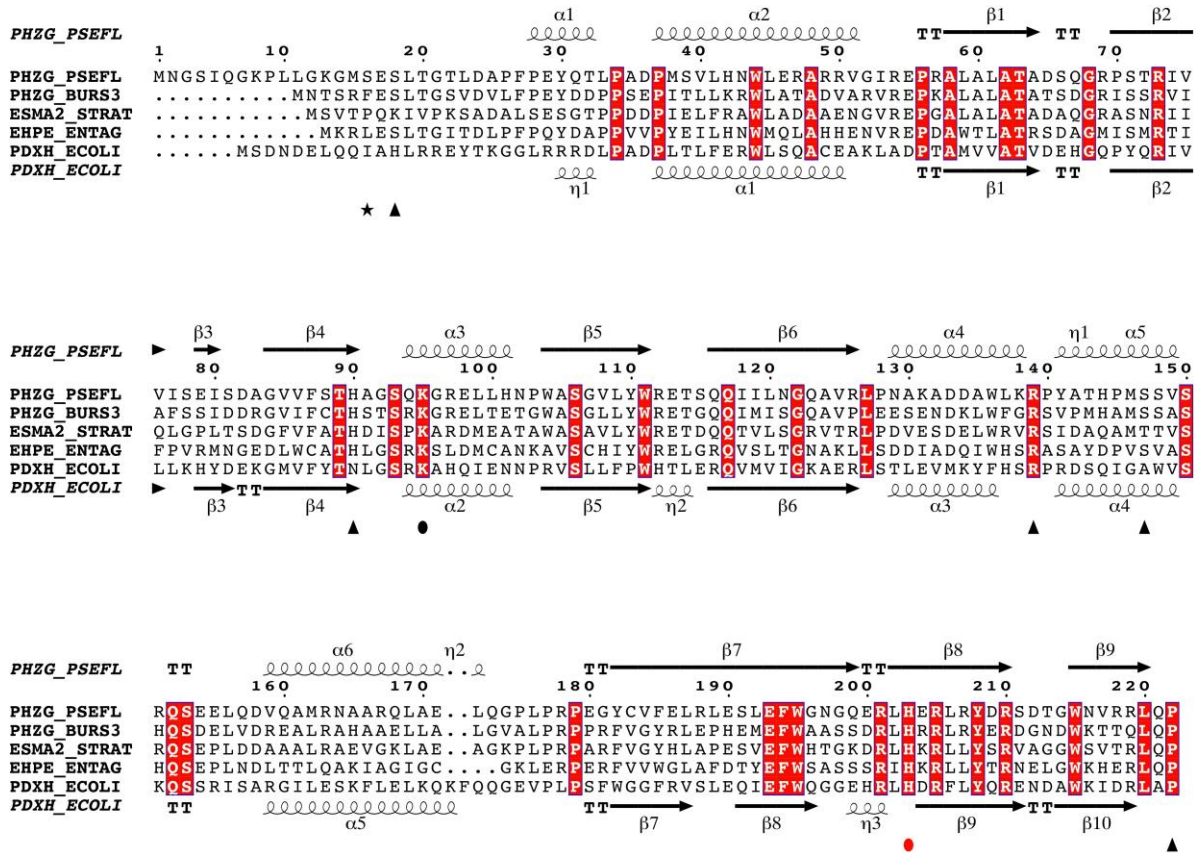
Correspondence email: wulf.blankenfeldt@uni-bayreuth.de

Figure S1



Stereo plots of $1\sigma |2FO - FC|$ electron density maps of the cofactor FMN and bound ligands in crystals of PhzG from *Pseudomonas fluorescens* 2-79 at the end of the refinement.

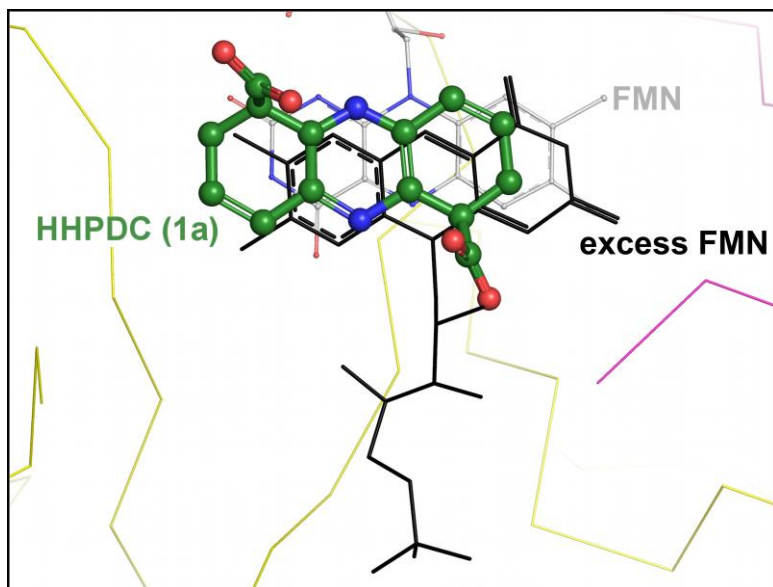
Figure S2



Structure-based sequence alignment of PhzGs from *Pseudomonas fluorescens* 2-79 (PHZG_PSEFL, Uniprot entry Q51793), *Burkholderia lata* 383 (PHZG_BURS3, Uniprot entry Q396C5), *Streptomyces antibioticus* Tü 2706 (ESMA2_STRAT; Uniprot entry H6ACX8_STRAT) and *Enterobacter agglomerans* Eh1087 (EHPE_ENTAG, Uniprot entry Q8GPH1_ENTAG) with pyridoxine 5'-phosphate oxidase PdxH from *E. coli* (PDXH_ECOLI, Uniprot entry P0AFI7). Secondary structure elements of *P. fluorescens* 2-79 PhzG (PDB entry 1TY9, (Parsons et al., 2004)) and *E. coli* PdxH (PDB entry 1G79, (Safo et al., 2001)) are shown on top and at the bottom of each block.

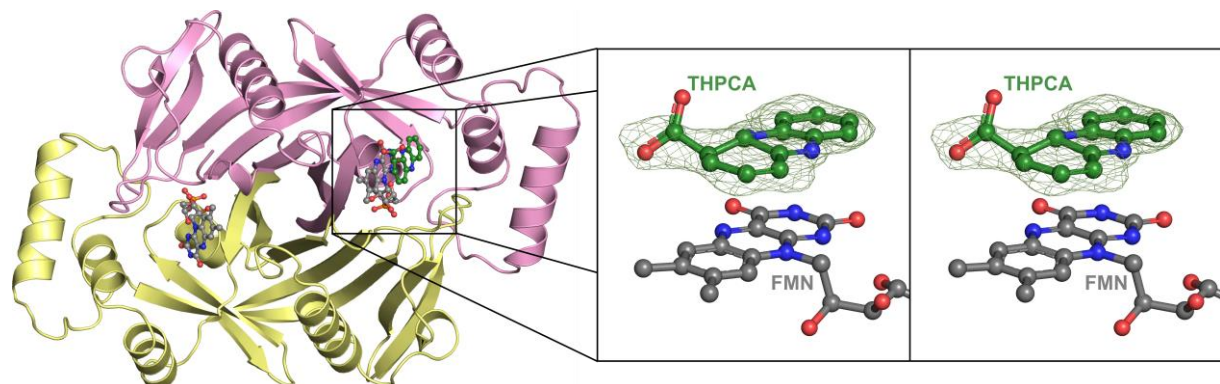
A star marks the first N-terminal residue visible in the electron density of *P. fluorescens* 2-79 PhzG in complex with hexahydro-phenazine-1,6-dicarboxylic acid (HHPDC, see main text). Black triangles indicate residues involved in the binding of HHPDC, red and black spheres mark residues postulated to be directly or indirectly involved in the enzymatic mechanism of PhzG, respectively (see Fig. 5C of the main text). The sequences were aligned with PROMALS3D (Pei et al., 2008) and rendered with ESPript (Gouet et al., 2003).

Figure S3



Superimposition of *P. fluorescens* 2-79 PhzG complexes with HHPDC (green) and excess FMN (thin black lines).

Figure S4



Crystal structure of PhzG from *Burkholderia lata* 383 in complex with tetrahydro-phenazine-1-carboxylic acid (THPCA). The magnified insert shows a stereo plot of $3 \sigma |FO - FC|$ difference electron density of the ligand before incorporation into the structural model.

Table S1 Data collection statistics for *Burkholderia lata* 383 PhzG

Values in parentheses are for the highest resolution shell. Both data sets were collected from single crystals on beamline X10SA of the Swiss Light Source (Paul Scherrer Institute, Villigen, Switzerland).

Dataset	Apo-structure	complex with intermediate 2a
Wavelength (Å)	0.99988	0.97886
Resolution range (Å)	47 – 1.53 (1.56 – 1.53)	47 – 1.59 (1.62 – 1.59)
Space group	P3 ₁	P3 ₁
Unit cell parameters (Å)	94.42, 94.42, 51.75	93.65, 93.65, 51.41
Mosaicity (°) [†]	0.323	0.169
Total No. of measured reflections	339919 (14939)	385105 (14994)
Unique reflections	77682 (3888)	67792 (3389)
Multiplicity	4.4 (3.8)	5.7 (4.4)
Mean I/σ(I)	10.1 (2.0)	16.0 (2.1)
Completeness (%)	99.7 (99.9)	99.9 (100)
R _{meas} (%) [‡]	8.7 (87.4)	6.3 (80.5)
R _{pim} (%) [§]	3.6 (44.6)	2.6 (38.1)

[†]Mosaicity values reported by XDS (Kabsch, 2010)

[‡]R_{meas} = $\sum_{hkl} (N/(N-1))^{1/2} \sum_i |I_i(hkl) - \langle I(hkl) \rangle| / \sum_{hkl} \sum_i I_i(hkl)$, where N is the number of observations of the reflection with index hkl and I_i is the intensity of its ith observation.

[§]R_{pim} = $\sum_{hkl} (1/(N-1))^{1/2} \sum_i |I_i(hkl) - \langle I(hkl) \rangle| / \sum_{hkl} \sum_i I_i(hkl)$ (Weiss, 2001).

Table S2 Refinement statistics for *Burkholderia lata* 383 PhzG

Values in parentheses are for the highest resolution shell.

Dataset	Apo-structure	complex with intermediate 2a
Resolution range (Å)	47 – 1.53 (1.55 – 1.53)	47 – 1.59 (1.61 – 1.59)
R _{cryst} (%)	13.3 (26.0)	11.3 (20.7)
R _{free} (%)	17.9 (30.6)	15.8 (27.0)
No. of non-H atoms		
Protein	3621	3569
Ion	-	-
Ligand	68	85
Water	544	490
R.m.s. deviations		
Bonds (Å)	0.012	0.019
Angles (°)	1.360	1.702
Average B factors (Å ²)		
Protein	27	25
Ion	-	-
Ligand	16	20
Water	39	39
Ramachandran plot		
Favoured regions (%)	98.3	98.0
Outliers (%)	0	0
MolProbity score [#]	1.31	1.34
PDB entry code	4HMW	4HMX

[#]As reported by MolProbity at <http://molprobity.biochem.duke.edu/> (Chen et al., 2010)

Supporting references

- Chen, V. B., Arendall, W. B., Headd, J. J., Keedy, D. A., Immormino, R. M., Kapral, G. J., Murray, L. W., Richardson, J. S., & Richardson, D. C. (2010). *Acta Crystallogr. D Biol. Crystallogr.* **66**, 12–21.
- Gouet, P., Robert, X., & Courcelle, E. (2003). *Nucleic Acids Research*. **31**, 3320–3323.
- Kabsch, W. (2010). *Acta Crystallogr. D Biol. Crystallogr.* **66**, 125–132.
- Parsons, J. F., Calabrese, K., Eisenstein, E., & Ladner, J. E. (2004). *Acta Crystallogr. D Biol. Crystallogr.* **60**, 2110–2113.
- Pei, J., Kim, B.-H., & Grishin, N. V. (2008). *Nucleic Acids Res.* **36**, 2295–2300.
- Safo, M. K., Musayev, F. N., Di Salvo, M. L., & Schirch, V. (2001). *J. Mol. Biol.* **310**, 817–826.
- Weiss, M. S. (2001). *Journal of Applied Crystallography*. **34**, 130–135.